New Computation of the Resonant Frequency of a Tunable Equilateral Triangular Microstrip Patch

Çiğdem Seçkin Gürel, *Student Member, IEEE,* and Erdem Yazgan, *Member, IEEE*

***Abstract*—A new dynamic permittivity expression is formulated to be used in the cavity analysis to determine the resonant frequency of an equilateral triangular microstrip patch. The proper sidelength extension expressions are given for low and high substrate permittivity cases. Better accuracy with respect to the moment method and other previous models is obtained for various structural parameters and operational modes. The proposed computation is also extended for the analysis of the two-layer structure in order to determine the air-gap tuning effect on the resonant frequency.**

***Index Terms*—Microstrip structures, resonant frequency.**

I. Introduction

HE triangular microstrip patch finds extensive applications in the design of many useful microwave integrated-circuit components such as circulators, resonators, and filters due to its high Q factor property [1], [2]. The same structure has also been used as an antenna having similar radiation properties to that of the rectangular patch with the advantage of small size and the disadvantage of narrow bandwidth [3]–[10]. The equilateral triangular microstrip patch is the most commonly used type of the triangular microstrip patches. In order to improve the efficiency of this structure, it is important to operate it around its resonant frequency. Various studies have been performed for the determination of the resonant frequencies of the equilateral triangular microstrip structures [1]–[10]. In those studies, the moment method and cavity model are widely used. The moment method, due to its accuracy and the adaptability to the multilayered structures, and the cavity model, due to its simplicity, have been preferred. Although the moment method provides accurate results for the calculation of resonant frequencies of the single and multilayered structures, it requires a large computational time. In the cavity analysis, the structure is modeled with a resonant cavity having electric walls on the top and bottom, and a magnetic wall around the sides. The proper effective values of the patch sidelength and substrate permittivity are required to correct the perfect magnetic-wall assumption. In some of the studies in the literature depending on the cavity analysis, it is preferred to use only the effective patch sidelength expression without changing the substrate permittivity [3]–[5]. Theories that suggest the usage of effective values for both substrate permittivity and patch sidelength are also present [6], [8]–[10]. The latest studies show that the last approach provides more accurate results if effective values for both permittivity and sidelength can be chosen correctly. In this study, it will be shown that, by replacing the effective permittivity value with the dynamic one, the results of the previous models can be improved. This can be explained with the inclusion of fringe field and inhomogenous modal field distribution effects in the dynamic permittivity expression. The proper sidelength extension formulas are also given in order to improve the accuracy of the calculations corresponding to low and high substrate permittivity cases.

The resonant frequency value of the equilateral triangular microstrip patch depends on the structural parameters, and it cannot be changed without manufacturing a new structure. In order to achieve tunable resonant frequency characteristic, an adjustable air-gap layer can be inserted between the ground plane and substrate, resulting in a two-layer structure. In this study, the dynamic permittivity expression formulated for the single-layer structure is extended for the two-layer case in order to determine the air-gap tuning effect on the resonant frequency, which has not been determined in previous studies presented in the literature.

The resonant frequency of the single-layer structure evaluated for the first five modes are compared with the available experimental and theoretical results. It is shown that an extra improvement over the results of the moment method and the various forms of the cavity analyses are obtained for most of the cases. The agreement between the theory and experiment is also very good, having an average percentage error (APE) value around 0.5%. The resonant frequencies corresponding to a two-layer structure are also presented for different gap widths.

II. Determination of the Resonant Frequency

The cavity model depending on the perfect magnetic-wall assumption leads to a resonant frequency expression for a single-layer equilateral triangular microstrip patch depicted in Fig. 1, as given in [1]

$$f_{mnl} = \frac{2c}{3a(\epsilon_{r2})^{1/2}}(m^2 + mn + n^2)^{1/2} \tag{1}$$

where c is the velocity of light in free space, a is the patch sidelength, ϵ_{r2} is the substrate relative permittivity and m, n, and l are the integers that cannot be zero simultaneously.

In most of the cavity analyses of the triangular microstrip patch, the substrate relative permittivity in (1) is replaced with an effective permittivity in order to improve the accuracy of the model [8]–[10]. In fact, the modal effects must be included in

Manuscript received August 12, 1998; revised December 10, 1999. This work was supported in part by the Scientific and Technical Research Council of Turkey, by the Hacettepe University Research Foundation under Contract 97.T01.604.006 and by the Turkish State Planning Organization under Contract 98K 121710.

The authors are with the Department of Electrical and Electronics Engineering, Hacettepe University, 06532 Beytepe, Ankara, Turkey.

Publisher Item Identifier S 0018-9480(00)02066-4.

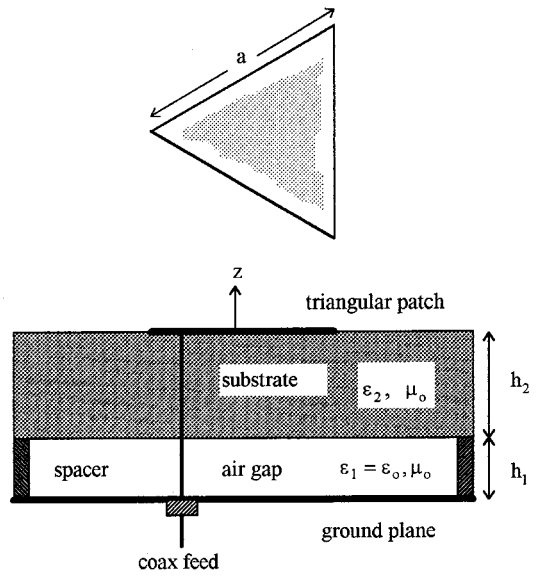

Fig. 1. Geometry of the tunable equilateral triangular microstrip patch.

the analysis that requires the usage of dynamic permittivity expression instead of an effective one. In this study, dynamic permittivity expression is obtained for a single- and two-layer triangular microstrip patch by using the equivalent models to determine all the necessary capacitance expressions. In order to give a general formulation for both single- and two-layer structures, the two-layer structure is modeled as the single-layer one having substrate thickness of $h = h_1 + h_2$ and an equivalent substrate relative permittivity of $\epsilon_{\rm req}$ determined under the cavity model approximations as

$$\epsilon_{\rm req} = \frac{\epsilon_{r2}(h_1 + h_2)}{(h_2 + \epsilon_{r2} h_1)}. \tag{2}$$

It is clear that the equivalent model reduces to the single-layer structure when the air-gap width is taken as $h_1 = 0$. In order to give a general dynamic permittivity expression, the structural parameters of the equivalent model are used as follows:

$$\epsilon_{\rm dyn} = \frac{C_{\rm dyn}(\epsilon_{ro}, \epsilon_{\rm req})}{C_{\rm dyn}(\epsilon_{ro} = \epsilon_{\rm req} = 1)} \tag{3}$$

where

$$C_{\rm dyn}(\epsilon_{\rm req}, \epsilon_{ro}) = C_{o,\rm dyn}(\epsilon_{\rm req}, \epsilon_{ro}) + C_{e,\rm dyn}(\epsilon_{\rm req}, \epsilon_{ro}). \tag{4}$$

In (4), $C_{e,\rm dyn}$ and $C_{o,\rm dyn}$ represent the total dynamic fringe and main field capacitances, respectively. In order to obtain the total dynamic fringe field capacitance $C_{c,\rm dyn}$, the equilateral triangular patch is replaced with a circular patch having an equivalent surface area. The radius of this circular patch is obtained as

$$r = (a^2 3^{0.5}/4\pi)^{1/2}. \tag{5}$$

The total dynamic fringe capacitance $C_{e,\rm dyn}$ of the original structure is taken in the form given in [11] as

$$C_{e,\rm dyn} = \frac{\epsilon_o \epsilon_{\rm req} A}{2h} C \tag{6}$$

where A is the physical area of the triangle and C is given by

$$C = \left\{1 + \frac{2h}{\pi \epsilon_{\rm req} r}\left[\ln\left(\frac{r}{2h}\right) + (1.41\epsilon_{\rm req} + 1.77) + \frac{h}{r}(0.268\epsilon_{\rm req} + 1.65)\right]\right\}^{1/2}. \tag{7}$$

The total dynamic main-field capacitance expression $C_{o,\rm dyn}$ for an equilateral triangular microstrip patch is taken in a similar form to that of the rectangular microstrip patch having the equivalent surface area [12] as

$$C_{o,\rm dyn} = C_{o,\rm stat}/\gamma_n \gamma_m \tag{8}$$

where $C_{o,\rm stat}$ is the static main capacitance given by

$$C_{o,\rm stat} = a^2 3^{0.5} \epsilon_o \epsilon_{\rm req}/4h \tag{9}$$

and

$$\gamma_{i(i=n,m)} = \begin{cases} 1, & i = 0 \\ 2, & i \neq 0. \end{cases}$$

The dynamic permittivity value can be determined from (2)–(9) and used in (1) instead of ϵ_{r2} in order to improve the accuracy of the resonant frequency calculation.

In order to include the fringe field effects, the patch sidelength in (1) must be replaced with the effective sidelength a_c. In the literature, various approximations have been used to represent the effective patch sidelength expression of the single layer structure [7]–[10]. One of those approximations was obtained by using the radius extension expression of the circular patch having the same surface area with the triangular patch [8] as

$$a_c = 2r_c \pi^{0.5}/3^{0.25} \tag{10}$$

where r_c represents the effective radius expression of the circular patch given in [8].

In this analysis, r_c is modified for a two-layer structure by assuming that the field is concentrated inside the upper dielectric layer and taken as

$$r_c = r\left\{1 + \frac{2h}{\pi \epsilon_{r2} r}\left[\ln\left(\frac{r}{2h}\right) + (1.41\epsilon_{r2} + 1.77) + \frac{h}{r}(0.268\epsilon_{r2} + 1.65)\right]\right\}^{1/2} \tag{11}$$

where h and ϵ_{r2} represent the total thickness and the substrate relative permittivity, respectively.

Another expression for an effective patch sidelength expression of the single-layer structure was given in a simpler form in [10] as

$$a_e = a + h\left(1.2 + \frac{2.25}{\sqrt{\epsilon_{\rm eff}}}\right) \tag{12}$$

where $\epsilon_{\rm eff}$ was defined as the effective substrate permittivity, which is taken in this study as

$$\epsilon_{\rm eff} = \frac{1}{2}(\epsilon_{r2} + 1) + \frac{1}{2}(\epsilon_{r2} - 1)\left(1 + \frac{12h}{(3^{0.25} a/2)}\right)^{-1/2}. \tag{13}$$

TABLE I
COMPARISON OF MEASURED AND NORMALIZED THEORETICAL RESONANT FREQUENCIES. $a = 10$ cm, $\epsilon_{r2} = 2.32$, $h_1 = 0$, $h_2 = 1.59$ mm

Mode:	f_{meas}, MHz [7]	f_{HJ} [1]	f_{GL} [4]	f_{XG} [6]	f_{CL1} [7]	f_{CL2} [7]	f_{KG} [8]	f_{KK} [9]	f_{DK} [10]	f_{GY}
TM_{10}	1280	1.015	0.995	1.047	1.006	1.013	1.000	1.007	1.001	0.998
TM_{11}	2242	1.004	0.983	1.035	1.008	1.001	0.989	0.996	0.990	0.992
TM_{20}	2550	1.019	0.998	1.051	1.024	1.016	1.004	1.011	1.005	1.002
TM_{21}	3400	1.011	0.991	1.042	1.016	1.008	0.996	1.003	0.997	0.999
TM_{30}	3824	1.020	0.999	1.051	1.013	1.016	1.004	1.012	1.005	1.003
APE (%):		1.39	0.67	4.51	1.33	1.08	0.46	0.74	0.48	0.30

TABLE II
COMPARISON OF MEASURED AND NORMALIZED THEORETICAL RESONANT FREQURNCIES. $a = 8.7$ cm, $\epsilon_{r2} = 10.5$, $h_1 = 0$, $h_2 = 0.7$ mm

Mode:	f_{meas}, MHz [7]	f_{HJ} [1]	f_{GL} [4]	f_{XG} [6]	f_{CL1} [7]	f_{CL2} [7]	f_{KG} [8]	f_{KK} [9]	f_{DK} [10]	f_{GY}
TM_{10}	1489	1.007	0.994	1.029	1.006	1.006	0.998	1.003	1.000	0.997
TM_{11}	2596	1.001	0.988	1.022	1.005	0.999	0.991	0.996	0.993	0.994
TM_{20}	2969	1.011	0.997	1.032	1.007	1.009	1.001	1.005	1.003	1.000
TM_{21}	3968	1.001	0.987	1.022	1.002	0.999	0.991	0.995	0.993	0.993
TM_{30}	4443	1.013	0.999	1.035	1.008	1.011	1.003	1.008	1.006	1.003
APE (%):		0.66	0.67	2.80	0.57	0.57	0.48	0.50	0.44	0.37

TABLE III
COMPARISON OF MEASURED AND NORMALIZED THEORETICAL RESONANT FREQUENCIES. $a = 4.1$ cm, $\epsilon_{r2} = 10.5$, $h_1 = 0$, $h_2 = 0.7$ mm

Mode:	f_{meas}, MHz [7]	f_{HJ} [1]	f_{GL} [4]	f_{XG} [6]	f_{CL1} [7]	f_{CL2} [7]	f_{KG} [8]	f_{KK} [9]	f_{DK} [10]	f_{GY}	f^{*}_{GY}
TM_{10}	1519	0.986	0.984	1.038	1.002	0.993	0.995	0.981	0.988	0.991	0.986
TM_{11}	2637	0.984	0.981	1.036	1.006	0.991	0.992	0.979	0.986	0.997	0.984
TM_{20}	2995	1.001	0.998	1.053	1.010	1.008	1.009	0.995	1.003	1.006	1.000
TM_{21}	3973	0.998	0.995	1.050	1.016	1.005	1.006	0.992	0.999	1.003	0.997
TM_{30}	4439	1.012	1.010	1.066	1.018	1.020	1.021	1.007	1.015	1.018	1.012
APE (%):		0.90	1.04	4.85	1.05	0.96	0.97	1.20	0.86	0.76	0.84

In this study, if substrate relative permittivity satisfies the $\epsilon_{r2} < 10$ condition, (10) is selected to represent an effective sidelength expression in order to improve the accuracy of the calculations. If ϵ_{r2} takes higher values and structure operates at the higher order modes, (12) is found to be better in order to satisfy the best fit with the experiments. The resonant frequency values are then determined from (1) by replacing the physical patch sidelength a and the substrate relative permittivity ϵ_{r2} with proper effective patch sidelength expression a_e and the dynamic permittivity expression $\epsilon_{\rm dyn}$, respectively.

III. COMPARISON OF THEORY AND EXPERIMENT

In order to verify the validity and accuracy of the proposed method, experimental and normalized theoretical resonant frequencies available in literature are presented in Tables I–III for

TABLE IV
COMPARISON OF THE NORMALIZED THEORETICAL RESONANT FREQUENCIES FOR HIGH SUBSTRATE PERMITTIVITY VALUE AND SEVERAL SUBSTRATE THICKNESSES. TM_{10} MODE, $a = 10$ cm, $\epsilon_{r2} = 10.0$, $h_1 = 0$

h_2 (mm)	f_{meas}, MHz [7]	f_{HJ}/f_{mom} [1]	f_{GL}/f_{mom} [4]	f_{XG}/f_{mom} [6]	f_{KG}/f_{mom} [8]	f_{DK}/f_{mom} [10]	f_{GY}/f_{mom}
4	639	0.977	0.975	1.062	0.989	0.973	0.980
8	631	0.978	0.977	1.098	0.983	0.951	0.970
12	619	0.985	0.989	1.129	0.977	0.928	0.964
16	608	0.991	1.000	1.152	0.966	0.903	0.957

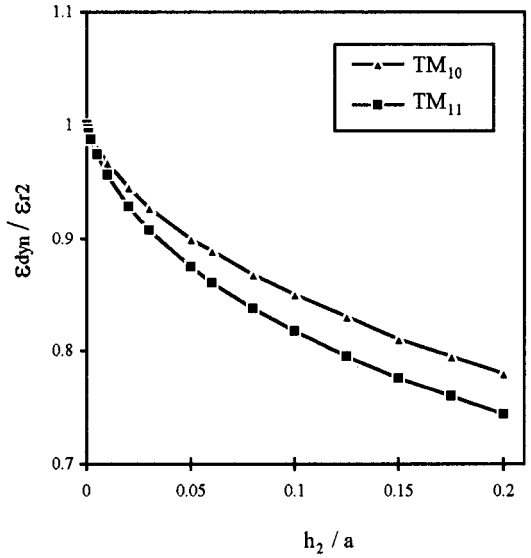

Fig. 2. Change of the normalized dynamic permittivity of the structure for TM_{10} and TM_{11} modes as a function of the h_2/a ratio. $h_1 = 0$, $\epsilon_{r2} = 6.4$.

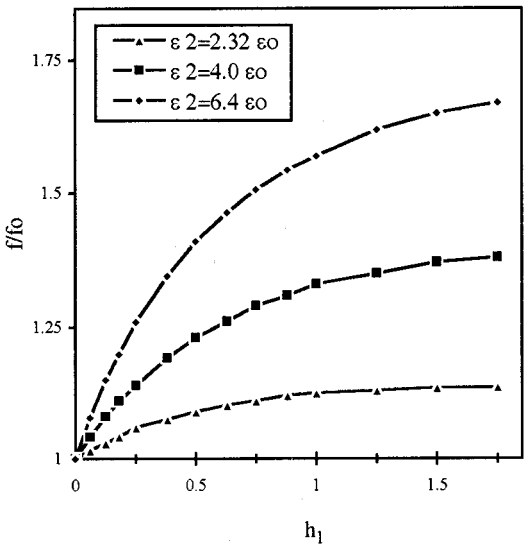

Fig. 3. Normalized resonant frequency shift for TM_{10} mode as a function of the air gap thickness h_1. $a = 4.0$ cm, $h_2 = 1.8$ mm.

different structural parameters and for the first five modes of an equilateral triangular microstrip patch. In these tables, the

TABLE V
THEORETICAL RESONANT FREQUENCIES (IN MEGAHETZ) FOR AN AIR-GAP TUNED STRUCTURE. $a = 10$ cm, $\epsilon_{r2} = 2.32$, $h_2 = 1.59$ mm

Mode:	$f_{r,nm}$ $h_1 = 0$	$f_{r,nm}$ $h_1 = 0.5$mm	$f_{r,nm}$ $h_1 = 1.0$mm
TM_{10}	1278	1436	1509
TM_{11}	2224	2486	2613
TM_{20}	2556	2871	3018
TM_{21}	3398	3798	3992
TM_{30}	3834	4307	4526

experimental results provided by Chen *et al.* [7] are shown as f_{meas}, the theoretical results provided by Helszajn and James [1] as f_{HJ}, by Garg and Long [4] as f_{GL}, by Gang [6] as f_{XG}, by Chen *et al.* [7] using the moment method and the cavity model as f_{CL1} and f_{CL2}, by Güney [8] as f_{KG}, by Karaboğa *et al.* [10] as f_{DK}, and the results of this study as f_{GY}, respectively. APE values are also shown as the final row of the each table. It is observed that the results obtained from the moment method are greater than the experimental values corresponding to the low and the high substrate permittivity cases. As is seen from Tables I–III, until this study, the results providing the best accuracy have been obtained by the theory of Garg and Long [4] by using a new effective sidelength expression, by the theory of Güney [8] by using a combination of the effective substrate permittivity and the effective sidelength expressions, and by the theory of Karaboğa *et al.* [10] by using a new and simple patch sidelength extension expression. In this study, by using a combination of the dynamic permittivity and the proper effective sidelength expressions, the results of the previous theories are improved having an APE value around 0.5%. In Table III, it is observed that the accuracy of the results tends to decrease if the substrate permittivity is high and the structure operates at the higher order modes. In order to decrease the percentage error values corresponding to these cases, (12) is found to be better as the effective patch sidelength expression. New results produced by using (12) instead of (10) are presented in the last column of Table III as f^{*}_{GY}, which provide better accuracy, especially for the higher order modes such as TM_{20}, TM_{21}, and TM_{30}. Thus, it can be concluded that the selection of this new sidelength extension formula for these specific cases will provide better results in the determination of the resonant frequencies. In Table IV, the resonant frequency results presented in some of the previous studies are given in the normalized form corresponding to several substrate thicknesses. It is observed that the results of this model are lower than that of the moment method, as in the previous cases.

In Fig. 2, the change of the normalized dynamic permittivity with the normalized substrate thickness is given for TM_{10} and TM_{11} modes. It is observed that the dynamic permittivity value approaches the substrate permittivity for thin substrates, and decreases with increasing substrate thickness. It is also observed that dynamic permittivity values corresponding to the TM_{10} mode are lower than that of the TM_{11} mode case. A similar

behavior is valid for the other operational modes depending on the mode index values.

All of the models mentioned above have not been modified for the determination of resonant frequency of the air-gap tuned triangular microstrip patch. In this study, a general formulation is presented for the two-layer structure, which has the air gap as one of the layers. The resonant frequencies corresponding to the three different gap widths are presented in Table V. In order to determine the air-gap tuning effect on the resonant frequency, the normalized resonant frequency shift with the air-gap thickness is shown for different substrate permittivities in Fig. 3. It is clear that the effect of the air-gap width on the resonant frequency increases for the high substrate permittivity values, which can be explained with the dependence of the equivalent relative permittivity expression on the air gap and substrate parameters.

IV. Conclusion

The resonant frequency of an equilateral triangular microstrip patch is determined from the cavity model by using a new dynamic permittivity expression combined with the proper sidelength extension formula. The method of computation produces the most accurate results to date for the fundamental and higher order modes. Therefore, it can be concluded that by using the dynamic permittivity expression in the calculations, instead of the effective one, better results with respect to the moment method and other present forms of the cavity analysis can be obtained. In this study, the computation is also extended for the two-layer structure in order to determine the air-gap tuning effect on the resonant frequency. It is expected that by using the developed new dynamic permittivity expression, the air-gap tuning effects on the other operational characteristics of the two-layer structure will also be determined accurately in future studies.

References

[1] J. Helszajn and D. S. James, "Planar triangular resonators with magnetic walls," *IEEE Trans. Microwave Theory Tech.*, vol. MTT-26, pp. 95–100, Feb. 1978.

[2] A. K. Sharma and B. Bhat, "Analysis of triangular microstrip resonators," *IEEE Trans. Microwave Theory Tech.*, vol. MTT-30, pp. 2029–2031, Nov. 1982.

[3] J. S. Dahele and K. F. Lee, "On the resonant frequencies of the triangular patch antenna," *IEEE Trans. Antennas Propagat.*, vol. AP-35, pp. 100–101, Jan. 1987.

[4] R. Garg and S. A. Long, "An improved formula for the resonant frequency of the triangular microstrip patch antenna," *IEEE Trans. Antennas Propagat.*, vol. AP-36, p. 570, Apr. 1988.

[5] R. Singh, A. De, and R. S. Yadava, "Comments on 'An improved formula for the resonant frequency of the triangular microstrip patch antenna," *IEEE Trans. Antennas Propagat.*, vol. 39, pp. 1443–1444, Sept. 1991.

[6] X. Gang, "On the resonant frequencies of microstrip antennas," *IEEE Trans. Antennas Propagat.*, pp. 245–247, Feb. 1989.

[7] W. Chen, K. F. Lee, and J. S. Dahele, "Theoretical and experimental studies of the resonant frequencies of equilateral triangular microstrip antenna," *IEEE Trans. Antennas Propagat.*, vol. 40, pp. 1253–1256, Oct. 1992.

[8] K. Güney, "Resonant frequency of a triangular microstrip antenna," *Microwave Opt. Technol. Lett.*, vol. 6, pp. 555–557, July 1993.

[9] N. Kumprasert and K. W. Kiranon, "Simple and accurate formula for the resonant frequency of the equilateral triangular microstrip patch antenna," *IEEE Trans. Antennas Propagat.*, vol. 42, pp. 1178–1179, Aug. 1994.

[10] D. Karaboğa, K. Güney, N. Karaboğa, and A. Kaplan, "Simple and accurate effective sidelength expression obtained by using a modified genetic algorithm for the resonant frequency of an equilateral triangular microstrip antenna," *Int. J. Electron.*, vol. 83, pp. 99–108, Jan. 1997.

[11] W. C. Chew and J. A. Kong, "Effects of fringing field on the capacitance of circular microstrip disk," *IEEE Trans. Microwave Theory Tech.*, vol. MTT-28, pp. 98–104, Feb. 1980.

[12] A. K. Verma and Z. Rostamy, "Resonant frequency of uncovered and covered rectangular microstrip patch using modified Wolff model," *IEEE Trans. Microwave Theory Tech.*, vol. MTT-41, pp. 109–116, Jan. 1980.

Çiğdem Seçkin Gürel (S'94) received B.S. and M.S. degrees in electrical engineering from the Hacettepe University, Ankara, Turkey, in 1991 and 1995, respectively, and is currently working toward the Ph.D. degree at Hacettepe University.

Since 1991, she has been a Research Assistant in the Department of Electrical Engineering, Hacettepe University. Her current research interests include antennas, multilayered structures, and microwave integrated circuits.

Erdem Yazgan (M'91) received the B.S. and M.S. degrees from the Middle East Technical University, Ankara, Turkey, in 1971 and 1973, respectively, and the Ph.D. degree from the Hacettepe University, Ankara, Turkey, in 1980, all in electrical engineering.

Since 1990, she has been a Professor in the Department of Electrical Engineering, Hacettepe University. In 1989, she was a Visiting Professor at Essex University, Essex, U.K. In 1994, she was a Visiting Professor in the Electroscience Laboratory, Ohio State University, Colombus. Her research interests include high-frequency (HF) propagation, low-altitude radar systems, reflector and microstrip antennas, microwave integrated-circuit design, Gaussian beam solutions, and medical electronics.